Methods to reduce power dissipation and supply voltage of LCD drivers

Raghavasimhan Thirunarayanan
Temkar N. Ruckmongathan

(SID Senior Member)

Abstract — Methods to reduce the power dissipation and supply voltage of LCD drivers for several line-by-line addressing techniques (*viz.*, addressing based on Hadamard matrices, diagonal matrices, and wavelets) are proposed, based on the analysis and estimation of power dissipation in the drivers. Power dissipation, supply voltage, number of time intervals required to address the display, and maximum number of voltage levels in the addressing waveforms of these techniques are compared with that of the Successive Approximation Technique.

1 Introduction

Power dissipation is an important figure of merit for liquid-crystal displays (LCDs). Power dissipation of LCDs depends on several physical parameters of the display, the image that is displayed and the addressing technique. A comparison of power dissipation of several addressing techniques is useful when selecting an addressing technique to drive the display. Our main objective in this paper is to analyze and estimate the average power dissipation of several line-by-line addressing techniques that can display gray shades and to reduce power dissipation and supply voltage by modifying the addressing waveforms. We have introduced two new techniques based on energy multiplexing[1] using Hadamard matrices and diagonal matrices.[2] Further, we have compared wavelet addressing[3] and two new techniques with the Successive Approximation Technique.[4] Power dissipation of the Successive Approximation Technique has been analyzed elsewhere[5]; however, it is included here as a reference to evaluate the relative performance of the other line-by-line addressing techniques. A general description of the energy-multiplexing technique is presented in the following section.

2 Generalized description of energy multiplexing

The gray shades of pixels is represented as a binary number and the gray-shade bits of each pixel are multiplexed using orthogonal functions. Let $O_i(t)$, where $i = 1 \ldots g$, denote the 'g' orthogonal functions. The orthogonal functions are chosen such that their amplitudes satisfy the following condition:

$$\int_0^T \left(k_i \cdot O_i(t)\right)^2 dt = 2^i, \tag{1}$$

where k_i is the scaling factor.

Let us consider a matrix display with N rows and M columns. Rows in the matrix display are selected one at a time with a select waveform that is proportional to the sum of orthogonal functions and is shown here:

$$W_{\text{row–sel}} \propto \sum_{i=1}^{g} k_i \cdot O_i(t) = V_r \cdot \sum_{i=1}^{g} k_i \cdot O_i(t). \tag{2}$$

Here, V_r is the constant of proportionality and is the factor that is used to vary the amplitude of the row waveforms. The waveform that is applied to each column in the matrix display is proportional to the multiplexed signal of the gray-shade bits of pixel in the selected row and in that column as shown in the following equation:

$$W_{\text{column–sel}} \propto \sum_{i=1}^{g} d_i \cdot k_i \cdot O_i(t) = V_c \cdot \sum_{i=1}^{g} d_i \cdot k_i \cdot O_i(t). \tag{3}$$

wherein d_i is the data corresponding to gray-shade bit-i of a pixel in the selected row and V_c is the constant of proportionality; d_i is assigned +1 if bit-i is logic-0 and –1 if it is logic-1. The waveform across a pixel during the select time is the difference of the row and column waveforms:

$$W_{\text{sel}} = W_{\text{row–sel}} - W_{\text{column–sel}} =$$
$$V_r \cdot \sum_{i=1}^{g} k_i \cdot O_i(t) - V_c \cdot \sum_{i=1}^{g} d_i \cdot k_i \cdot O_i(t). \tag{4}$$

The waveform across the pixel when it is not selected ($W_{\text{non-sel}}$) is obtained by substituting $V_r = 0$ in the above equation because the non-select voltage is zero. Thus, the rms voltage across a pixel is

$$V_{RMS} = \sqrt{\frac{1}{NT}\left(\int_0^T (W_{\text{sel}})^2 dt + (N-1) \cdot \int_0^T (W_{\text{non–sel}})^2 dt\right)}. \tag{5}$$

Orthogonal functions are also represented in a matrix of the form $O_{r \times l}$. For displaying 'g' gray shades, 'g' orthogo-

nal functions can be selected from the orthogonal matrix. Let $o_{i,j}$ denote an element of the orthogonal matrix (where i varies from 1 to 'g' and j from 1 to 'l') and k_i be the scaling factor. Then, the select and non-select voltages across the pixels during the time interval 'j' are as follows:

$$w_{\text{sel},j} = \left(V_r \sum_{i=1}^{g} k_i o_{i,j} - V_c \sum_{i=1}^{g} d_i k_i o_{i,j} \right), \qquad (6)$$

$$w_{\text{sel},j} = \left(V_r S_j - V_c D_j \right), \qquad (7)$$

wherein

$$S_j = \sum_{i=1}^{g} k_i o_{i,j} \text{ and } D_j = \sum_{i=1}^{g} d_i k_i o_{i,j},$$

$$w_{\text{non-sel},j} = \left(V_c \sum_{i=1}^{g} d_i k_i o_{i,j} \right) = V_c D_j. \qquad (8)$$

The expression for the rms voltage across a pixel is as follows:

$$\sqrt{\frac{\sum_{j=1}^{l} \left(V_r S_j - V_c D_j \right)^2 + (N-1) \sum_{j=1}^{l} \left(D_j V_c \right)^2}{l \cdot N}}. \qquad (9)$$

The rms voltage across an ON pixel is obtained when a value of '-1' is assigned to all the gray-shade bits. Therefore, if $\forall i$, $d_i = -1$, then $D_j = -S_j$:

$$V_{ON}(RMS) = \sqrt{\frac{\sum_{j=1}^{l} \left(S_j (V_r + V_c) \right)^2 + (N-1) \sum_{j=1}^{l} (S_j V_c)^2}{l, N}}. \qquad (10)$$

Similarly, the rms voltage across an OFF pixel is obtained by assigning a '$+1$' to all the gray-shade bits.

$$V_{OFF}(RMS) = \sqrt{\frac{\sum_{j=1}^{l} \left(S_j (V_r - V_c) \right)^2 + (N-1) \sum_{j=1}^{l} (S_j V_c)^2}{l, N}}. \qquad (11)$$

The selection ratio, the ratio of the rms voltage across ON pixels to that across OFF pixels, is a maximum when $V_r = N^{1/2} V_c$, and the maximum selection ratio is

$$\frac{V_{ON}(RMS)}{V_{OFF}(RMS)} = \sqrt{\frac{\sqrt{N}+1}{\sqrt{N}-1}}. \qquad (12)$$

The amplitude of the row and column waveforms depends on the electro-optic characteristics of the display. The contrast between the ON and OFF pixels is maximum when the rms voltage of the OFF pixel is near the threshold voltage of the display, *i.e.*, V_{th}. Therefore, the rms voltage across OFF pixels is equated to V_{th}, the threshold voltage of the display from which the proportionality constant V_c can be computed as shown here:

$$V_c = V_{th} \cdot \sqrt{\frac{l \cdot N}{\sum_{j=1}^{l} S_j^2 \cdot 2(N - \sqrt{N})}}. \qquad (13)$$

The supply voltage is determined by the maximum swing in the addressing waveform, and can be reduced either by shifting the pulses or inverting the polarity of the instantaneous voltages of both row and column voltages during some of the intervals as discussed in later part of this paper.

The use of diagonal-matrices multi-line addressing techniques has been demonstrated previously.[6] Here, we have illustrated the line-by-line addressing technique based on diagonal matrices by an example given below. For example, let us consider the diagonal matrix of order 8 given in matrix (14):

$$\begin{bmatrix} -3 & 1 & 1 & 1 & 1 & 1 & 1 & 1 \\ 1 & -3 & 1 & 1 & 1 & 1 & 1 & 1 \\ 1 & 1 & -3 & 1 & 1 & 1 & 1 & 1 \\ 1 & 1 & 1 & -3 & 1 & 1 & 1 & 1 \\ 1 & 1 & 1 & 1 & -3 & 1 & 1 & 1 \\ 1 & 1 & 1 & 1 & 1 & -3 & 1 & 1 \\ 1 & 1 & 1 & 1 & 1 & 1 & -3 & 1 \\ 1 & 1 & 1 & 1 & 1 & 1 & 1 & -3 \end{bmatrix} \qquad (14)$$

Elements in each row of the matrix are multiplied by $k_i = (2^{1/2})^{g-i}$ so that the energy of the waveform corresponding to each row is proportional to one bit of gray shade. Thus, the modified orthogonal matrix for displaying gray shades is shown in matrix (15):

$$\begin{bmatrix} -24\sqrt{2} & 8\sqrt{2} & 8\sqrt{2} & 8\sqrt{2} & 8\sqrt{2} & 8\sqrt{2} & 8\sqrt{2} & 8\sqrt{2} \\ 8 & -24 & 8 & 8 & 8 & 8 & 8 & 8 \\ 4\sqrt{2} & 4\sqrt{2} & -12\sqrt{2} & 4\sqrt{2} & 4\sqrt{2} & 4\sqrt{2} & 4\sqrt{2} & 4\sqrt{2} \\ 4 & 4 & 4 & -12 & 4 & 4 & 4 & 4 \\ 2\sqrt{2} & 2\sqrt{2} & 2\sqrt{2} & 2\sqrt{2} & -6\sqrt{2} & 2\sqrt{2} & 2\sqrt{2} & 2\sqrt{2} \\ 2 & 2 & 2 & 2 & 2 & -6 & 2 & 2 \\ \sqrt{2} & \sqrt{2} & \sqrt{2} & \sqrt{2} & \sqrt{2} & \sqrt{2} & -3\sqrt{2} & \sqrt{2} \\ 1 & 1 & 1 & 1 & 1 & 1 & 1 & -3 \end{bmatrix} \qquad (15)$$

Select pulses (denoted by $S_j V_r$) are obtained by the column-wise sum of elements in the orthogonal matrix of matrix (15) as shown here:

$$\left(15 - 17\sqrt{2}\right) \cdot V_r, \left(15\sqrt{2} - 17\right) \cdot V_r, \left(15 - \sqrt{2}\right) \cdot V_r, \left(15\sqrt{2} - 1\right) \cdot V_r,$$
$$\left(15 + 7\sqrt{2}\right) \cdot V_r, \left(15\sqrt{2} + 7\right) \cdot V_r, \left(15 + 11\sqrt{2}\right) \cdot V_r, \left(15\sqrt{2} + 11\right) \cdot V_r. \qquad (16)$$

Let us consider an arbitrary gray shade, for example, (01101011); the data vector corresponding to this gray shade is obtained by assigning +1 for logic 0 and –1 for logic 1 for the binary bits:
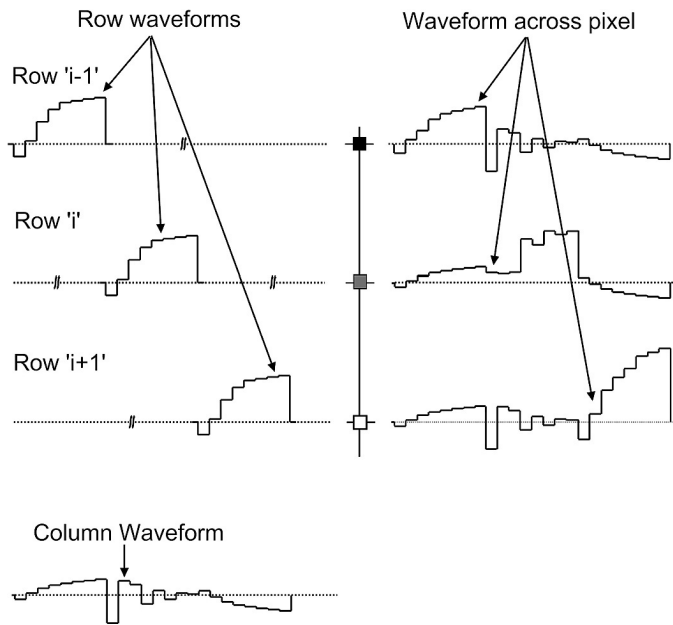
Row waveforms

Row 'i-1'

Row 'i'

Row 'i+1'

Waveform across pixel

Column Waveform

FIGURE 1 — Typical waveforms for the addressing technique based on a diagonal matrix of order 8.

and the display is refreshed continuously by repeating this cycle at a rate that is fast enough to avoid flicker. The typical waveforms for the addressing illustrated above are shown in Fig. 1.

A similar procedure can be followed for displaying gray shades using Hadamard matrices and wavelets. The addressing techniques using diagonal matrices, Hadamard matrices, and wavelets use both time and amplitude modulation to display gray shades. The Successive Approximation Technique is the only technique in which just the amplitude modulation is used. The select pulses of the Successive Approximation Technique for 3–12 bits of gray shade are shown in Table 1. Select pulses for 8–4096 gray shades that are based on Hadamard matrices are shown in Table 2. Similarly, select pulses that are based on diagonal matrices are shown in Table 3. Select pulses corresponding to the wavelets are shown in Table 4, followed by an illustration of the estimation of power dissipation and supply voltage. The orthogonal matrices used in the wavelet-based addressing technique are shown in the Appendix.

$$\langle +1,-1,-1,+1,-1,+1,-1,-1 \rangle. \tag{17}$$

Pulses in the data waveform are obtained by multiplying the transpose of the modified matrix shown in matrix (15) with the data vector in expression (17). The resulting pulses in the data waveform are as follows:

$$\left(-3-31\sqrt{2}\right)\cdot V_c, \left(\sqrt{2}+29\right)\cdot V_c, \left(17\sqrt{2}-3\right)\cdot V_c, \left(\sqrt{2}-19\right)\cdot V_c,$$
$$\left(9\sqrt{2}-3\right)\cdot V_c, \left(\sqrt{2}-11\right)\cdot V_c, \left(5\sqrt{2}-3\right)\cdot V_c, \left(\sqrt{2}+1\right)\cdot V_c. \tag{18}$$

The select pulses in expression (16) and the data pulses given in expression (18) are applied sequentially to the pixel. A cycle is completed when all the N rows in a matrix display are selected once with all the select pulses,

TABLE 1 — Select pulses of successive approximation technique.

No. of gray shades	Select pulses
8	$\left(2, \sqrt{2}, 1\right)V_r$
16	$\left(2\sqrt{2}, 2, \sqrt{2}, 1\right)V_r$
32	$\left(4, 2\sqrt{2}, 2, \sqrt{2}, 1\right)V_r$
64	$\left(4\sqrt{2}, 4, 2\sqrt{2}, 2, \sqrt{2}, 1\right)V_r$
128	$\left(8, 4\sqrt{2}, 4, 2\sqrt{2}, 2, \sqrt{2}, 1\right)V_r$
256	$\left(8\sqrt{2}, 8, 4\sqrt{2}, 4, 2\sqrt{2}, 2, \sqrt{2}, 1\right)V_r$
512	$\left(16, 8\sqrt{2}, 8, 4\sqrt{2}, 4, 2\sqrt{2}, 2, \sqrt{2}, 1\right)V_r$
1024	$\left(16\sqrt{2}, 16, 8\sqrt{2}, 8, 4\sqrt{2}, 4, 2\sqrt{2}, 2, \sqrt{2}, 1\right)V_r$
2048	$\left(32, 16\sqrt{2}, 16, 8\sqrt{2}, 8, 4\sqrt{2}, 4, 2\sqrt{2}, 2, \sqrt{2}, 1\right)V_r$
4096	$\left(32\sqrt{2}, 32, 16\sqrt{2}, 16, 8\sqrt{2}, 8, 4\sqrt{2}, 4, 2\sqrt{2}, 2, \sqrt{2}, 1\right)V_r$

TABLE 2 — Select pulses of Hadamard-matrix-based addressing technique.

No. of gray shades	Select pulses
8	$\left((\sqrt{2}+3), (\sqrt{2}+1), (1-\sqrt{2}), (3-\sqrt{2})\right)\cdot V_r$
16	$\left((3\sqrt{2}+3), (\sqrt{2}+1), (\sqrt{2}-1), (3\sqrt{2}-3)\right)\cdot V_r$
32	$\begin{pmatrix}(3\sqrt{2}+7), (3\sqrt{2}+5), (\sqrt{2}+1), (\sqrt{2}+3), \\ (3-\sqrt{2}), (1-\sqrt{2}), (5-3\sqrt{2}), (7-3\sqrt{2})\end{pmatrix}\cdot V_r$
64	$\begin{pmatrix}(7+7\sqrt{2}), (5+5\sqrt{2}), (1+\sqrt{2}), (3+3\sqrt{2}), \\ (3\sqrt{2}-3), (\sqrt{2}-1), (5\sqrt{2}-5), (7\sqrt{2}-7)\end{pmatrix}\cdot V_r$
128	$\begin{pmatrix}(7\sqrt{2}+15), (5\sqrt{2}+9), (\sqrt{2}+3), (3\sqrt{2}+5), \\ (5-3\sqrt{2}), (3-\sqrt{2}), (9-5\sqrt{2}), (15-7\sqrt{2})\end{pmatrix}\cdot V_r$
256	$\begin{pmatrix}(15\sqrt{2}+15), (9\sqrt{2}+9), (3+3\sqrt{2}), (5+5\sqrt{2}), \\ (5\sqrt{2}-5), (3\sqrt{2}-3), (9\sqrt{2}-9), (15\sqrt{2}-15)\end{pmatrix}\cdot V_r$
512	$\begin{pmatrix}(15\sqrt{2}+31), (15\sqrt{2}+29), (9\sqrt{2}+17), (9\sqrt{2}+19), \\ (3\sqrt{2}+7), (3\sqrt{2}+5), (5\sqrt{2}+9), (5\sqrt{2}+11), \\ (11-5\sqrt{2}), (9-5\sqrt{2}), (5-3\sqrt{2}), (7-3\sqrt{2}), \\ (19-9\sqrt{2}), (17-9\sqrt{2}), (29-15\sqrt{2}), (31-15\sqrt{2})\end{pmatrix}\cdot V_r$
1024	$\begin{pmatrix}(31\sqrt{2}+31), (29\sqrt{2}+29), (17\sqrt{2}+17), (19\sqrt{2}+19), \\ (7\sqrt{2}+7), (5\sqrt{2}+5), (9\sqrt{2}+9), (11\sqrt{2}+11), \\ (11\sqrt{2}-11), (9\sqrt{2}-9), (5\sqrt{2}-5), (7\sqrt{2}-7), \\ (19\sqrt{2}-19), (17\sqrt{2}-17), (29\sqrt{2}-29), (31\sqrt{2}-31)\end{pmatrix}\cdot V_r$
2048	$\begin{pmatrix}(31\sqrt{2}+63), (29\sqrt{2}+57), (17\sqrt{2}+33), (19\sqrt{2}+39), \\ (7\sqrt{2}+13), (5\sqrt{2}+11), (9\sqrt{2}+19), (11\sqrt{2}+21), \\ (21-11\sqrt{2}), (19-9\sqrt{2}), (11-5\sqrt{2}), (13-7\sqrt{2}), \\ (39-19\sqrt{2}), (33-17\sqrt{2}), (57-29\sqrt{2}), (63-31\sqrt{2})\end{pmatrix}\cdot V_r$
4096	$\begin{pmatrix}(63\sqrt{2}+63), (57\sqrt{2}+57), (33\sqrt{2}+33), (39\sqrt{2}+39), \\ (13\sqrt{2}+13), (11\sqrt{2}+11), (19\sqrt{2}+19), (21\sqrt{2}+21), \\ (21\sqrt{2}-21), (19\sqrt{2}-19), (11\sqrt{2}-11), (13\sqrt{2}-13), \\ (39\sqrt{2}-39), (33\sqrt{2}-33), (57\sqrt{2}-57), (63\sqrt{2}-63)\end{pmatrix}\cdot V_r$

TABLE 3 — Select pulses of diagonal-matrix-based addressing technique.

No. of gray shades	Select pulses
8	$\left(\left(2\sqrt{2}\right),\ \left(6-\sqrt{2}\right),\ \left(3+2\sqrt{2}\right)\right)\cdot V_r$
16	$\left(\left(3-\sqrt{2}\right),\ \left(3\sqrt{2}-1\right),\ \left(3+\sqrt{2}\right),\ \left(1+3\sqrt{2}\right)\right)\cdot V_r$
32	$\left(\begin{array}{l}(-6+6\sqrt{2}),\ (14-4\sqrt{2}),\ (6\sqrt{2}+4),\ (\sqrt{2}+14),\\ (9+6\sqrt{2})\end{array}\right)\cdot V_r$
64	$\left(\begin{array}{l}(7-5\sqrt{2}),\ (-5+7\sqrt{2}),\ (7+\sqrt{2}),\ (1+7\sqrt{2}),\\ (7+4\sqrt{2}),\ (4+7\sqrt{2})\end{array}\right)\cdot V_r$
128	$\left(\begin{array}{l}(-26+14\sqrt{2}),\ (30-14\sqrt{2}),\ (2+14\sqrt{2}),\ (30),\\ (16+14\sqrt{2}),\ (30+7\sqrt{2}),\ (23+14\sqrt{2})\end{array}\right)\cdot V_r$
256	$\left(\begin{array}{l}(15-17\sqrt{2}),\ (-17+15\sqrt{2}),\ (15-\sqrt{2}),\ (15\sqrt{2}-1),\\ (15+7\sqrt{2}),\ (7+15\sqrt{2}),\ (15+11\sqrt{2}),\ (11+15\sqrt{2})\end{array}\right)\cdot V_r$
512	$\left(\begin{array}{l}(-82+30\sqrt{2}),\ (62-42\sqrt{2}),\ (-10+30\sqrt{2}),\ (62-6\sqrt{2}),\\ (26+30\sqrt{2}),\ (62+12\sqrt{2}),\ (44+30\sqrt{2}),\ (62+2\sqrt{2}),\\ (53+30\sqrt{2})\end{array}\right)\cdot V_r$
1024	$\left(\begin{array}{l}(31-49\sqrt{2}),\ (-49+31\sqrt{2}),\ (31-9\sqrt{2}),\ (-9+31\sqrt{2}),\\ (31+11\sqrt{2}),\ (11+31\sqrt{2}),\ (31+21\sqrt{2}),\ (21+31\sqrt{2}),\\ (31+26\sqrt{2}),\ (26+31\sqrt{2})\end{array}\right)\cdot V_r$
2048	$\left(\begin{array}{l}(-226+62\sqrt{2}),\ (126-114\sqrt{2}),\ (-50+62\sqrt{2}),\ (126-26\sqrt{2}),\\ (38+62\sqrt{2}),\ (126+18\sqrt{2}),\ (82+62\sqrt{2}),\ (126+40\sqrt{2}),\\ (104+62\sqrt{2}),\ (126+51\sqrt{2}),\ (115+62\sqrt{2})\end{array}\right)\cdot V_r$
4096	$\left(\begin{array}{l}(63-129\sqrt{2}),\ (-129+63\sqrt{2}),\ (63-33\sqrt{2}),\ (-33+63\sqrt{2}),\\ (63+15\sqrt{2}),\ (15+63\sqrt{2}),\ (63+39\sqrt{2}),\ (39+63\sqrt{2}),\\ (51\sqrt{2}+63),\ (51+63\sqrt{2}),\ (63+57\sqrt{2}),\ (57+63\sqrt{2}\end{array}\right)\cdot V_r$

Note: The proportionality constant V_r is presented outside the braces as a common factor in Tables 1–4 due to space constraint.

TABLE 4 — Select pulses of wavelet-based addressing technique.

No. of gray shades	Select pulses
8	$\left(\left(\sqrt{2}+1\right),\ \left(\sqrt{2}+1\right),\ \sqrt{2},\ \left(-2+\sqrt{2}\right)\right)\cdot V_r$
16	$\left(\left(2\sqrt{2}+2\right),\ 2,\ \left(3-\sqrt{2}\right),\ \left(1-\sqrt{2}\right)\right)\cdot V_r$
32	$\left(\begin{array}{l}(3+\sqrt{2}),\ (3+\sqrt{2}),\ (\sqrt{2}+1),\ (\sqrt{2}+1),\\ 2,\ 2,\ (3-2\sqrt{2}),\ (1-2\sqrt{2})\end{array}\right)\cdot V_r$
64	$\left(\begin{array}{l}(2+2\sqrt{2}),\ (2+2\sqrt{2}),\ (4+2\sqrt{2}),\ (2\sqrt{2}),\\ (3\sqrt{2}),\ (\sqrt{2}),\ (-3+2\sqrt{2}),\ (-5+2\sqrt{2})\end{array}\right)\cdot V_r$
128	$\left(\begin{array}{l}(4+4\sqrt{2}),\ (4+4\sqrt{2}),\ 6,\ 2,\ (6-\sqrt{2}),\\ (6-3\sqrt{2}),\ (3-2\sqrt{2}),\ (1-2\sqrt{2})\end{array}\right)\cdot V_r$
256	$\left(\begin{array}{l}(4\sqrt{2}+8),\ (4\sqrt{2}+4),\ (6+2\sqrt{2}),\ (2+2\sqrt{2}),\\ (5\sqrt{2}),\ (3\sqrt{2}),\ (-7+4\sqrt{2}),\ (-9+4\sqrt{2})\end{array}\right)\cdot V_r$
512	$\left(\begin{array}{l}16,\ 8,\ (12+2\sqrt{2}),\ (12-2\sqrt{2}),6,\ 2,\ (4+\sqrt{2}),\\ (4-\sqrt{2}),12,\ 12,\ 5,\ 3\end{array}\right)\cdot V_r$
1024	$\left(\begin{array}{l}(8+8\sqrt{2}),\ \ (8+8\sqrt{2}),\ (8\sqrt{2}-4),\ (8\sqrt{2}-12),\\ 14\sqrt{2},\ 10\sqrt{2},\ (4\sqrt{2}+2),\ (4\sqrt{2}-2),\\ (9\sqrt{2}+4),\ (7\sqrt{2}+4),\ \ (8\sqrt{2}-3),\ (8\sqrt{2}-5)\end{array}\right)\cdot V_r$
2048	$\left(\begin{array}{l}10\sqrt{2},\ 10\sqrt{2},\ 6\sqrt{2},\ 6\sqrt{2},\ (-12+8\sqrt{2}),\\ (-12+8\sqrt{2}),(-20+8\sqrt{2}),\ (-20+8\sqrt{2}),(8+14\sqrt{2}),\\ (8+10\sqrt{2}),(4\sqrt{2}+10),\ (4\sqrt{2}+6),\ (16+9\sqrt{2}),\\ (16+7\sqrt{2}),\ (8\sqrt{2}+1),\ (8\sqrt{2}-1)\end{array}\right)\cdot V_r$
4096	$\left(\begin{array}{l}(4\sqrt{2}+16),(16-4\sqrt{2}),\ 20,\ 12,(16-12\sqrt{2}),\\ (16-12\sqrt{2}),\ (16-20\sqrt{2}),\ (16-20\sqrt{2}),(10\sqrt{2}+24),\\ (24+6\sqrt{2}),(10+8\sqrt{2}),\ (6+8\sqrt{2}),(16+17\sqrt{2}),\\ (16+15\sqrt{2}),\ 17,\ 15\end{array}\right)\cdot V_r$

3 Estimation of power dissipation in drivers

A matrix LCD is modeled as an array of capacitors[7] for analyzing power dissipation in the drivers of the matrix display. The power consumed in the driver circuit is the sum of power dissipated in the digital part of the driver circuit (*viz.*, shift registers and latches) and the analog part of the drive circuit. Our analysis is confined to power dissipation in the analog part of the driver circuit, *i.e.*, the power, which is dissipated in the resistors (ON resistance of the switch in the drivers and resistance of indium tin oxide electrodes in the display) when addressing waveforms are applied to capacitive-type pixels in the display. Although the matrix display can be modeled as an array of capacitors, the capacitance of the pixel depends on state of the pixel because the dielectric constant of the liquid crystal sandwiched between the electrodes of the pixel depends on the voltage across the pixel. Hence, the power dissipation will depend on the actual image that is displayed. In our analysis, we have assumed that each gray shade has the same probability of occurrence and an average capacitance is assigned to all the pixels irrespective of its state. The power dissipation occurs in the resistance of the drive circuit during the transitions in the addressing waveforms. Let $S_j \cdot V_r$ and $D_j \cdot V_c$ (S_j and D_j have been defined in the previous section) be the select and data pulses that are applied to a pixel during the time interval j and the voltage across the pixel during this time interval is $S_j V_r - D_j V_c$. Similarly, the voltage across the pixel during the time interval $j + 1$ will be $S_{j+1}V_r - D_{j+1}V_c$ and the voltage transition across the pixel will be $(S_{j+1} - S_j)V_r - (D_{j+1} - D_j)V_c$. Hence, the power dissipated in the resistance of the driver circuit is proportional to the following expression:

$$\left[(S_{j+1} - S_j)V_r - (D_{j+1} - D_j)V_c\right]^2. \tag{19}$$

Thus, the power dissipation due to a transition in the waveform across the pixel is

$$p_j \propto \left(\begin{matrix} \left(S_{j+1}-S_j\right)^2 V_r^2 + \left(D_{j+1}-D_j\right)^2 V_c^2 \\ -2\left(S_{j+1}-S_j\right)\left(D_{j+1}-D_j\right)V_r V_c \end{matrix} \right). \quad (20)$$

Power dissipated during all the transitions in the select waveform is the summation of transitions, wherein $S_0 = S_{l+1} = 0$, $i.e.$, the select voltage is zero in the beginning and end of select waveform. Let l be the number of pulses in the select waveform, then the total power dissipation during the select time is proportional to the following expression:

$$\left(\begin{matrix} V_r^2 \left(\sum_{j=1}^{l} S_j^2 - \sum_{j=1}^{l-1} S_j S_{j+1} \right) + V_c^2 \left(\sum_{j=1}^{l} D_j^2 - \sum_{k=1}^{l-1} D_j D_{j+1} \right) \\ -V_r V_c \left(\sum_{k=1}^{l} 2 S_j D_j - \sum_{k=1}^{l-1} \left(S_j D_{j+1} + S_{j+1} D_j \right) \right) \end{matrix} \right). \quad (21)$$

Thus far, we have not made any assumption on the gray shade of the pixel; the expression of power dissipation will be same to complement the gray shade except for the sign of the third term, which will be opposite to that of a gray shade. Hence, the V_r^2 and V_c^2 terms will remain, whereas $V_r V_c$ will cancel when the average power dissipation of two gray shades that are the complement of each other is calculated. Thus, the average power dissipation will be proportional to the following expression:

$$\sum_{j=1}^{l} \left(S_j^2 V_r^2 + D_j^2 V_c^2 \right) - \sum_{j=1}^{l-1} \left(S_j S_{j+1} V_r^2 + D_j D_{j+1} V_c^2 \right). \quad (22)$$

Power dissipated in the resistances of the drivers when pixels in rest of the $(N-1)$ rows are selected can be obtained by substituting $V_r = 0$ as shown in the following expression:

$$(N-1)\left(\sum_{j=1}^{l} \left(D_j^2 V_c^2 \right) - \sum_{k=1}^{l-1} \left(D_j D_{j+1} V_c^2 \right) \right). \quad (23)$$

Hence, the power dissipated by displaying two complementary gray shades during a cycle will be proportional to the following expression:

$$\left(\sum_{j=1}^{l} \left(S_j^2 V_r^2 + N D_j^2 V_c^2 \right) - \sum_{j=1}^{l-1} \left(S_j S_{j+1} V_r^2 + N D_j D_{j+1} V_c^2 \right) \right). \quad (24)$$

Power dissipated for all the gray shades can be obtained by computing the above expression for the first $2^{(g-1)}$ gray shades. Further simplification of this general expression is possible only when specific orthogonal functions are considered, except for the substitution of $V_r = N^{1/2} V_c$, the condition for maximum selection ratio, as shown below:

$$N V_c^2 \left(\sum_{j=1}^{l} \left(S_j^2 + D_j^2 \right) - \sum_{j=1}^{l-1} \left(S_j S_{j+1} + D_j D_{j+1} \right) \right). \quad (25)$$

We have illustrated the estimation of power dissipation and supply voltage for the case of line-by-line address-
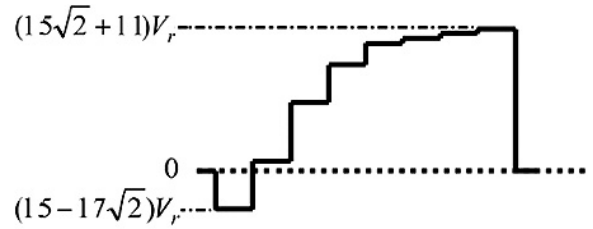
FIGURE 2 — Select waveform for displaying 256 gray shades using diagonal matrix.

ing using a diagonal matrix of order 8 shown previously in Sec. 3.

For ease of reference, we have reproduced the select and data waveforms (when gray shade 01101011 is being displayed) below:
Select waveform:

$$(15-17\sqrt{2})V_r, (15\sqrt{2}-17)V_r, (15-\sqrt{2})V_r, (15\sqrt{2}-1)V_r, \\ (15+7\sqrt{2})V_r, (15\sqrt{2}+7)V_r, (15+11\sqrt{2})V_r, (15\sqrt{2}+11)V_r. \quad (26)$$

The transitions in the select waveform $(S_{j+1} - S_j)$ are

$$(15-17\sqrt{2})V_r, (32\sqrt{2}-32)V_r, (32-16\sqrt{2})V_r, \\ (16\sqrt{2}-16)V_r, \\ (16-8\sqrt{2})V_r, (8\sqrt{2}-8)V_r, (8-4\sqrt{2})V_r, (4\sqrt{2}-4)V_r, \\ -(15\sqrt{2}+11)V_r. \quad (27)$$

The select waveform given in expression (26) has been shown in Fig. 2.
Data waveform:

$$(-3-31\sqrt{2})V_c, (\sqrt{2}+29)V_c, (17\sqrt{2}-3)V_c, (\sqrt{2}-19)V_c, \\ (9\sqrt{2}-3)V_c, (\sqrt{2}-11)V_c, (5\sqrt{2}-3)V_c, (\sqrt{2}+1)V_c. \quad (28)$$

The transitions in the data waveform $(D_{j+1} - D_j)$ are

$$(-3-31\sqrt{2})V_c, (32\sqrt{2}+32)V_c, (16\sqrt{2}-32)V_c, \\ (-16\sqrt{2}-16)V_c, \\ (8\sqrt{2}+16)V_c, (-8\sqrt{2}-8)V_c, (4\sqrt{2}+8)V_c, (-4\sqrt{2}+4)V_c, \\ (\sqrt{2}+1)V_c. \quad (29)$$

The power dissipated when a pixel in a row is proportional to expression (30) and is obtained by substituting the values for S_j and D_j in expression (24):

$$1408.08 V_r^2 + 11056.41 V_c^2 - 1274.69 V_r V_c. \quad (30)$$

Power dissipated during the select time for the complementary gray shade (10010100) is calculated by using a similar procedure and is proportional to the following expression:

$$1408.08 V_r^2 + 11056.41 V_c^2 + 1274.69 V_r V_c. \quad (31)$$

The V_rV_c term of complementary gray shades is cancelled when the average power dissipation is computed with the assumption that all gray shades are equally probable.

The average power dissipation is obtained by following a similar procedure for all gray shades, and the average power dissipation during the select time of a pixel is as follows:

$$1408.08V_r^2 + 7578V_c^2. \tag{32}$$

The average power dissipated while charging the pixel capacitor when other $(N-1)$ rows are selected is as follows:

$$(N-1)7578V_c^2. \tag{33}$$

Hence, the average power dissipated to charge and discharge a pixel as required by the addressing waveforms is proportional to the following expression:

$$1408.08V_r^2 + 7578NV_c^2. \tag{34}$$

Power dissipation is normalized to the threshold voltage (V_{th}) of the display and is obtained by substituting for V_c obtained by using Eq. (13):

$$V_c\sqrt{\frac{8N}{4080.2\cdot(N-\sqrt{N})}}\cdot V_{th}. \tag{35}$$

The average power dissipation is proportional to the following expression after substituting for $V_r{}^2$ and $V_c{}^2$ in Eq. (32):

$$8.8098\frac{N}{N-\sqrt{N}}\cdot V_{th}. \tag{36}$$

The supply voltage (V_s) is determined by the maximum swing in the addressing waveforms; *i.e.*, the maximum swing in the waveform across the pixel and it as follows:

$$V_s = (11+15\sqrt{2})V_r - (15-17\sqrt{2})V_r. \tag{37}$$

TABLE 5 — Comparison of average power dissipation of several addressing techniques.

No. of gray shades	Power dissipation normalized to that of successive approximation technique (in %)		
	Diagonal matrix	Hadamard	Wavelet
8	95.99	116.15	92.83
16	92.53	97.01	91.61
32	93.17	94.49	79.59
64	88.10	83.96	69.18
128	86.89	73.60	59.10
256	86.13	64.39	55.73
512	85.11	59.30	61.94
1024	85.55	54.39	61.54
2048	85.55	50.33	58.10
4096	85.69	46.42	54.75

The supply voltage after substituting for V_r and V_c is as follows:

$$V_s = 1.2917\sqrt{N}\cdot\sqrt{\frac{N}{N-\sqrt{N}}}\cdot V_{th}. \tag{38}$$

A comparison between the power dissipation of the techniques based on diagonal matrices, Hadamard matrices, and wavelets normalized to that of the power dissipation of the successive approximation is shown in Table 5.

4   Reducing power dissipation and supply voltage

The rms voltage across a pixel will be the same if the order of select pulses and the corresponding data pulses are paired up and rearranged; however, the power dissipation in the drivers will be different because the amplitude of transition will depend on the consecutive select and data pulses. The order of select pulses (and the corresponding data pulses) can be rearranged such that the select waveform is a discrete approximation of a triangle in the sense that the amplitude increases first and decreases after the peak pulse to reduce the power dissipation of the driver circuit. This approach is illustrated with the same example as in Sec. 3. Select pulses of expression (16) are rearranged to avoid large transitions between adjacent pulses. The new select waveform is given in expression (39) and is shown in Fig. 3.

$$(15-\sqrt{2})V_r, (15+7\sqrt{2})V_r, (15+11\sqrt{2})V_r, (11+15\sqrt{2})V_r,$$
$$(7+15\sqrt{2})V_r, (15\sqrt{2}-1)V_r, (15\sqrt{2}-17)V_r, (15-17\sqrt{2})V_r. \tag{39}$$

Here, the transitions in the select waveform is given below:

$$(15-\sqrt{2})V_r, (8\sqrt{2})V_r, (4\sqrt{2})V_r, (-4+4\sqrt{2})V_r, (-8)V_r,$$
$$(-8)V_r, (-16)V_r, (-32\sqrt{2}+32)V_r, -(17\sqrt{2}+15)V_r. \tag{40}$$

The procedure for the calculation of power dissipation is the same as shown in the previous section. The average power dissipation for the new sequence is proportional to

$$8.1674\frac{N}{N-\sqrt{N}}\cdot V_{th}^2. \tag{41}$$
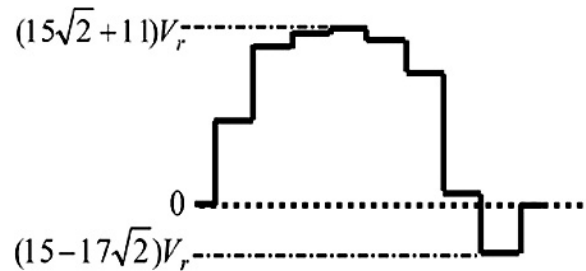
FIGURE 3 — Rearranged select waveform.

FIGURE 4 — Select waveform with inversion.

FIGURE 5 — Select waveform, inherently DC-free.

In some cases, for example, addressing based on diagonal matrices (for displaying 128 gray shades and above) and wavelets, the supply voltage will be high because the select waveforms have both positive and negative select pulses. In such cases, a reduction in supply voltage can be achieved either by shifting both the row and the column waveform by the desired amount[8] or by inverting the polarity of the negative select pulses and the corresponding data pulses. Both of these operations have the same effect and will not affect the rms voltage. In the case of our example, there is a large positive-to-negative swing in the waveform corresponding to the MSB leading to a high supply voltage. Both select and data pulses are inverted, and the pulses are rearranged in an ascending followed by descending pulses as given in expression (42). The select waveform with the polarity of the negative pulse inverted is shown in Fig. 4.

$$(15-\sqrt{2})V_r, (15+7\sqrt{2})V_r, (15+11\sqrt{2})V_r, (11+15\sqrt{2})V_r,$$
$$(7+15\sqrt{2})V_r, (15\sqrt{2}-1)V_r, (-15+17\sqrt{2})V_r, (15\sqrt{2}-17)V_r. \quad (42)$$

The transitions in the select waveform are given below:

$$(15-\sqrt{2})V_r, (8\sqrt{2})V_r, (4\sqrt{2})V_r, (-4+4\sqrt{2})V_r, (-8)V_r,$$
$$(-8)V_r, (-14+2\sqrt{2})V_r, (-2\sqrt{2}-2)V_r, -(15\sqrt{2}-17)V_r. \quad (43)$$

The reduced supply voltage for the select waveform shown in expression (42) is computed as follows:

$$V_s = (11+15\sqrt{2})V_r + (15+31\sqrt{2})V_c. \quad (44)$$

It simplifies to the following expression after substituting for V_r and V_c:

$$V_s = (1.0086\sqrt{N} + 1.8423) \cdot \sqrt{\frac{N}{N-\sqrt{N}}} \cdot V_{th}. \quad (45)$$

The supply voltage after the polarity inversion in the above equation is always less than that of the supply voltage expression given in Eq. (38) for $N > 1$.

A reduction of power dissipation is obtained by rearranging the modified waveform as shown previously in this section. The average power dissipation for this pulse is proportional to the following expression:

$$5.0580 \frac{N}{N-\sqrt{N}} \cdot V_{th}^2. \quad (46)$$

Thus, power dissipation is reduced to about 57% as that in expression (36). Hence, significant reductions in sup-

ply voltage and power dissipation are achieved by simple modification in the addressing waveforms.
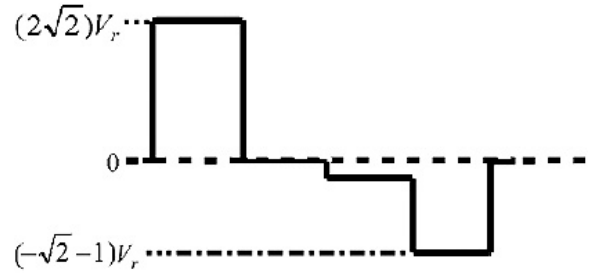
Waveform across the pixels should be DC-free to ensure long life of the display. One way to achieve this DC-free operation is to select orthogonal matrices such that all of its rows have both positive and negative voltage swings for equal time intervals. This operation leads to an increase in power dissipation due to the large voltage transitions in the waveform corresponding to the most significant bit (which has the highest energy). For example, let us consider the matrix given below, which is used for displaying eight gray shades using a wavelet-based addressing technique:

$$\begin{bmatrix} \sqrt{2} & \sqrt{2} & -\sqrt{2} & -\sqrt{2} \\ \sqrt{2} & -\sqrt{2} & 0 & 0 \\ 0 & 0 & 1 & -1 \end{bmatrix}. \quad (47)$$

The select waveform in this case is

$$2\sqrt{2}V_r, 0, (-\sqrt{2}+1)V_r, (-\sqrt{2}-1)V_r. \quad (48)$$

The above waveform is shown in Fig. 5.

Although the orthogonal matrix given in expression (47) is DC-free, it has a large positive-to-negative swing of amplitude of $2(2^{1/2})V_r$ in the waveform corresponding to MSB which increases the power dissipation.

The power dissipation in this case is computed to be

$$4 \cdot \frac{N}{N-\sqrt{N}} \cdot V_{th}^2. \quad (49)$$

Reducing the high-amplitude transition in the select waveform corresponding to the MSB will decrease power dissipation. An example of such a reduction is given below with the MSB of the orthogonal matrix in Eq. (50) having a DC component, while the other rows are DC-free:

$$\begin{bmatrix} \sqrt{2} & \sqrt{2} & \sqrt{2} & \sqrt{2} \\ \sqrt{2} & -\sqrt{2} & 0 & 0 \\ 0 & 0 & 1 & -1 \end{bmatrix}. \quad (50)$$

Here, the select waveform is given by

$$2\sqrt{2}V_r, 0, (\sqrt{2}+1)V_r, (\sqrt{2}-1)V_r. \quad (51)$$

The power dissipation calculated for this case is
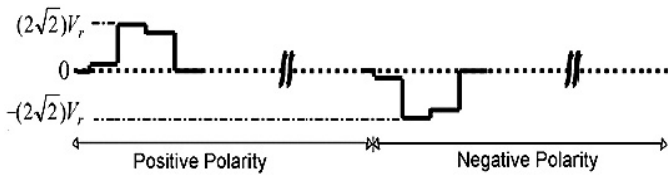
FIGURE 6 — Select waveform, polarity reversal.
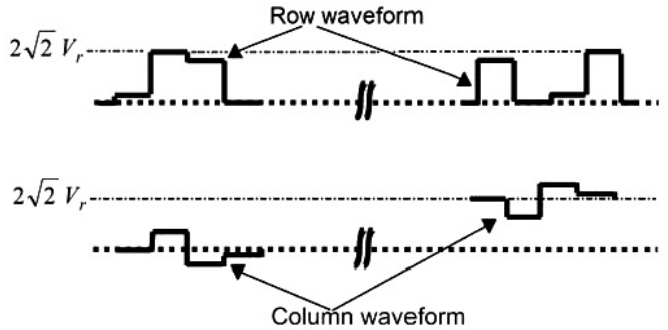
FIGURE 7 — Level-shifted row waveform and column waveform.
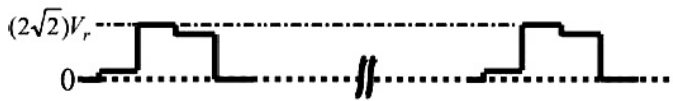
FIGURE 8 — Select waveform, level-shifted and rearranged.
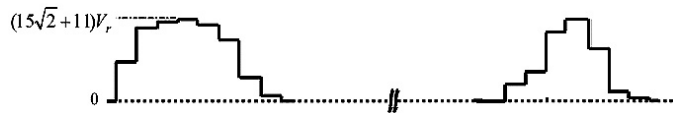
FIGURE 9 — Diagonal matrix-based addressing, Select waveform level-shifted and rearranged.

$$3.42 \cdot \frac{N}{N - \sqrt{N}} \cdot V_{th}^2. \tag{52}$$

Thus, this technique shows a decrease in power dissipation (in this case by 14.5%) compared to the other technique, which incorporates an inherent DC-free operation. Rearrangement of the select pulses (for reducing power dissipation) with ascending pulses followed by descending pulses is shown in expression (53):

$$(\sqrt{2} - 1)V_r,\ 2\sqrt{2}V_r,\ (\sqrt{2} + 1)V_r,\ 0. \tag{53}$$

The power dissipation in this case is

$$2.285 \frac{N}{N - \sqrt{N}} \cdot V_{th}^2. \tag{54}$$

To achieve a DC-free condition in the above example, the polarity of the select and the data waveforms are reversed for alternate select times. The rearranged select pulses with polarity reversal are shown in Fig. 6.

But the supply voltage is doubled when the polarity is reversed for DC-free operation. The supply voltage in this

case can be reduced by level shifting both the select and data pulses[8] by the same amount [a shift of $2(2^{1/2})V_r$ is used in this case]. The level-shifted row and column waveforms for the above example are shown in Fig. 7. The supply voltage for the case with level shifting is given by

$$V_s = 0.7559(\sqrt{N} + 1) \cdot \sqrt{\frac{N}{N - \sqrt{N}}} \cdot V_{th}.$$

Although there are large transitions at the beginning and at the end of the level-shifted pulses, the power dissipation will be same as that of the waveform with positive polarity since both the row and the data waveform are shifted by the same amount; the voltage across the pixels will not change. However, in practical circuits, the output resistances of the row and the column drivers will be different, resulting in a net voltage across the pixel even during transitions due to differences in the time constant of the row and column drivers and the difference in amplitude due to the data voltages. Rearranging the select pulses in ascending order followed by descending order as shown in Fig. 8 will reduce the error in the rms voltage due to the difference in the rise and fall times in the row and column waveforms.

A similar level-shifted and rearranged select waveform for the example of diagonal matrix-based addressing is given in Fig. 9.

TABLE 6 — Normalizing factor (V_c technique/V_c successive approximation).

No. of gray shades	Normalizing factor (V_e technique/V_e Successive Approximation)		
	Diagonal matrix	Hadamard matrix	Wavelet
8	$\dfrac{1}{3}$	$\dfrac{1}{\sqrt{3}}$	$\sqrt{\dfrac{2}{3}}$
16	$\dfrac{1}{2}$	$\dfrac{1}{\sqrt{4}}$	$\sqrt{\dfrac{1}{2}}$
32	$\dfrac{1}{5}$	$\dfrac{1}{\sqrt{5}}$	$\sqrt{\dfrac{4}{5}}$
64	$\dfrac{1}{3}$	$\dfrac{1}{\sqrt{6}}$	$\sqrt{\dfrac{2}{3}}$
128	$\dfrac{1}{7}$	$\dfrac{1}{\sqrt{7}}$	$\sqrt{\dfrac{4}{7}}$
256	$\dfrac{1}{4}$	$\dfrac{1}{\sqrt{8}}$	$\sqrt{\dfrac{1}{2}}$
512	$\dfrac{1}{9}$	$\dfrac{1}{\sqrt{9}}$	$\sqrt{\dfrac{2}{3}}$
1024	$\dfrac{1}{5}$	$\dfrac{1}{\sqrt{10}}$	$\sqrt{\dfrac{3}{5}}$
2048	$\dfrac{1}{11}$	$\dfrac{1}{\sqrt{11}}$	$\sqrt{\dfrac{8}{11}}$
4096	$\dfrac{1}{6}$	$\dfrac{1}{\sqrt{12}}$	$\sqrt{\dfrac{2}{3}}$

TABLE 7 — Select waveforms of Successive Approximation Technique.
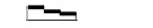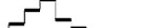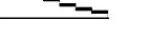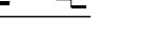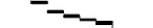
No. of gray shades	Select waveform	
	From orthogonal matrix	Low power
8		
16		
32		
64		
128		
256		
512		
1024		
2048		
4096		

TABLE 8 — Select waveforms of Hadamard-matrix-based technique.
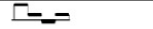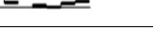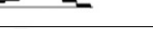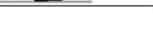
No. of gray shades	Select waveform	
	From orthogonal matrix	Low power
8		
16		
32		
64		
128		
256		
512		
1024		
2048		
4096		

TABLE 9 — Select waveforms of diagonal-matrix-based technique.
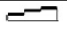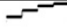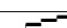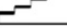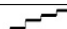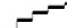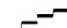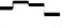
No. of gray shades	Select waveform	
	From orthogonal matrix	Low power
8		
16		
32		
64		
128		
256		
512		
1024		
2048		
4096		

TABLE 10 — Select waveforms of wavelet-based addressing technique.
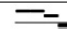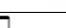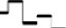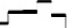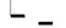
No. of gray shades	Select waveform	
	From orthogonal matrix	Low power
8		
16		
32		
64		
128		
256		
512		
1024		
2048		
4096		

TABLE 11 — Comparison of average power dissipation in drivers for several addressing techniques (after rearrangement).

No. of gray shades	Percentage Power dissipation with respect to successive approximation (after rearranging the pulses)		
	Diagonal matrix	Hadamard matrix	Wavelet
8	90.61	103.02	98.77
16	87.02	95.41	88.16
32	85.75	87.25	76.69
64	68.31	81.98	63.57
128	65.74	74.15	52.75
256	54.93	66.18	51.27
512	55.81	58.66	40.97
1024	66.77	57.57	41.81
2048	59.32	53.45	39.05
4096	60.28	49.26	31.64

TABLE 12 — Comparison of supply voltage of addressing techniques.

No. of gray shades	Percentage supply voltage with respect to successive approximation (after rearranging the pulses)*		
	Diagonal matrix	Hadamard matrix	Wavelet
8	100.16	127.42	98.55
16	95.92	128.04	120.71
32	91.59	125.69	98.70
64	86.53	121.96	98.55
128	81.46	117.64	91.25
256	76.55	113.16	95.71
512	71.90	108.77	81.67
1024	67.62	104.58	67.81
2048	63.64	100.66	76.55
4096	60.07	97.02	72.25

*For $N = 100$.

TABLE 13 — Comparison of time intervals required for addressing.

No. of gray shades	Time intervals required for addressing (in terms of N)			
	Successive approx.	Diagonal matrix	Hadamard matrix	Wavelet
8	3	3	4	4
16	4	4	4	4
32	5	5	8	8
64	6	6	8	8
128	7	7	8	8
256	8	8	8	8
512	9	9	16	12
1024	10	10	16	12
2048	11	11	16	16
4096	12	12	16	16

TABLE 14 — Comparison of maximum number of voltage levels in column waveform at any instant of time.

No. of gray shades	Maximum Number of voltage levels in column waveform at any instant of time			
	Successive approx.	Diagonal matrix	Hadamard matrix	Wavelet
8	2	8	8	8
16	2	16	16	8
32	2	32	32	14
64	2	64	64	16
128	2	128	128	16
256	2	256	256	16
512	2	512	512	8
1024	2	1024	1024	8
2048	2	2048	2048	16
4096	2	4096	4096	16

5 A comparison on various energy-multiplexing techniques

The unit amplitude of the data voltage V_c varies from technique to technique due to different waveform profiles. Hence, for comparison purposes, a normalizing factor (the ratio of V_c of the particular technique to V_c of the Successive Approximation Technique) is used. In this section, we have given the normalizing factors for the amplitude of select and data waveforms for various techniques in Table 6. We have also shown the waveforms derived from the orthogonal matrices and the modified waveforms for low power for the Successive Approximation Technique, addressing technique based on Hadamard matrices, diagonal matrix addressing, and wavelet-based addressing technique in Tables 7–10, respectively. Further, a comparison between the Successive Approximation Technique (which has been taken as the benchmark), addressing technique using Hadamard matrices, diagonal matrix addressing, and wavelet-based addressing technique based on parameters such as the power dissipation (low power) (Table 11), supply voltage (Table 12), number of time intervals required for addressing (Table 13), and the maximum number of voltage levels in the column waveform at any instant of time (Table 14) has been carried out.

6 Conclusion

Wavelet-based addressing has the lowest power dissipation as evident from the analysis, and a comparison of power dissipation shown in Table 11. Addressing techniques based on diagonal matrices have lower power dissipation compared to Hadamard matrices for up to 256 gray shades, while the latter has lower power dissipation for 512 or more gray shades. The supply voltage is the least for an addressing technique based on diagonal matrices. It is followed by the addressing techniques based on wavelets and Hadamard matrices. However, the column waveforms of the addressing techniques based on a diagonal matrix and Hadamard matrix

is proportional to the number of gray shades, *i.e.,* 2^g. Hence, the hardware complexity of column drivers will be high, whereas the wavelet-based technique has 16 or less number of voltages in the column waveforms up to 4096 gray shades. Further, power dissipation in drivers is less by 50–70% compared to the Successive Approximation Technique, when the wavelet-based line-by-line addressing technique is used for displaying 256 or more gray shades.

References

1. T. N. Ruckmongathan, "Techniques with low hardware complexity of driver electronics," *J. Soc. Info. Display* **15**, No. 12, 1121–1129 (2007).
2. T. N. Ruckmongathan, "Orthogonal matrices for multi-line addressing," *IEEE/OSA J.Display Technol.* **4**, No. 1, 6–8 (March 2008).
3. T. N. Ruckmongathan *et al.,* "Line-by-line addressing of RMS responding matrix displays with wavelets," *IEEE/OSA J. Display Technol.* **3**, No. 4, 413–420 (December 2007).
4. T. N. Ruckmongathan, "A successive approximation technique for displaying gray shades in liquid crystal displays (LCDs)," *IEEE Trans. Image Processing* **16**, No. 2, 554–561 (February 2007).
5. T. N. Ruckmongathan, "Low power techniques for gray shades in liquid crystal displays," *IEEE/OSA J. Display Technol.* **5**, No. 2, 49–56 (February 2009).
6. R. Gopalan and T. N. Ruckmongathan, "Multi-line addressing of LCDs with simple diagonal matrices," *SID Symposium Digest* **39**, 1873–1876 (2008).
7. B. W. Marks, "Power consumption of multiplexed liquid crystal displays," *IEEE Trans. Electron. Dev.* **ED-29**, No. 8, 1218–1222 (1982).
8. H. Kawakami *et al.,* "Matrix addressing technology of twisted nematic displays," *SID-IEEE Conference Record of the Biennial Display Research Conference,* 50–52 (1976).

Appendix
Orthogonal matrices used for the wavelet-addressing technique

Orthogonal matrix for 8 gray shades:

$$\begin{bmatrix} y & y & \bar{y} & \bar{y} \\ z & z & z & \bar{z} \\ 0 & 0 & z & \bar{z} \end{bmatrix} \quad \text{(a)}$$

Orthogonal matrix for 16 gray shades:

$$\begin{bmatrix} x & x & x & \bar{x} \\ y & y & \bar{y} & \bar{y} \\ y & \bar{y} & 0 & 0 \\ 0 & 0 & z & \bar{z} \end{bmatrix} \quad \text{(b)}$$

Orthogonal matrix for 32 gray shades:

$$\begin{bmatrix} x & x & x & x & \bar{x} & x & \bar{x} & \bar{x} \\ y & y & y & y & \bar{y} & \bar{y} & \bar{y} & \bar{y} \\ 0 & 0 & 0 & 0 & y & y & \bar{y} & \bar{y} \\ z & z & \bar{z} & \bar{z} & 0 & 0 & 0 & 0 \\ 0 & 0 & 0 & 0 & 0 & 0 & z & \bar{z} \end{bmatrix} \quad \text{(c)}$$

Orthogonal matrix for 64 gray shades:

$$\begin{bmatrix} w & w & w & w & \bar{w} & w & \bar{w} & \bar{w} \\ x & x & x & x & \bar{x} & x & \bar{x} & \bar{x} \\ 0 & 0 & 0 & 0 & x & x & x & x \\ 0 & 0 & x & \bar{x} & 0 & 0 & 0 & 0 \\ 0 & 0 & 0 & 0 & y & \bar{y} & 0 & 0 \\ 0 & 0 & 0 & 0 & 0 & 0 & z & \bar{z} \end{bmatrix} \quad \text{(d)}$$

Orthogonal matrix for 128 gray shades:

$$\begin{bmatrix} v & v & v & v & \bar{v} & \bar{v} & \bar{v} & \bar{v} \\ w & w & \bar{w} & \bar{w} & \bar{w} & \bar{w} & \bar{w} & \bar{w} \\ w & w & \bar{w} & \bar{w} & 0 & 0 & 0 & 0 \\ 0 & 0 & 0 & 0 & x & x & \bar{x} & \bar{x} \\ 0 & 0 & x & \bar{x} & 0 & 0 & 0 & 0 \\ 0 & 0 & 0 & 0 & y & \bar{y} & 0 & 0 \\ 0 & 0 & 0 & 0 & 0 & 0 & z & \bar{z} \end{bmatrix} \quad \text{(e)}$$

Orthogonal matrix for 256 gray shades:

$$\begin{bmatrix} d & d & d & d & \bar{d} & \bar{d} & \bar{d} & \bar{d} \\ v & v & v & v & \bar{v} & \bar{v} & \bar{v} & \bar{v} \\ 0 & 0 & 0 & 0 & v & v & \bar{v} & \bar{v} \\ w & w & \bar{w} & \bar{w} & 0 & 0 & 0 & 0 \\ w & \bar{w} & 0 & 0 & 0 & 0 & 0 & 0 \\ 0 & 0 & x & \bar{x} & 0 & 0 & 0 & 0 \\ 0 & 0 & 0 & 0 & y & \bar{y} & 0 & 0 \\ 0 & 0 & 0 & 0 & 0 & 0 & z & \bar{z} \end{bmatrix} \quad \text{(f)}$$

Orthogonal matrix for 512 gray shades:

$$\begin{bmatrix} c & c & c & c & c & c & c & c & 0 & 0 & 0 & 0 \\ 0 & 0 & 0 & 0 & \bar{0} & 0 & 0 & 0 & c & c & c & c \\ v & v & v & v & \bar{v} & \bar{v} & \bar{v} & \bar{v} & 0 & 0 & 0 & 0 \\ 0 & \bar{0} & 0 & 0 & 0 & 0 & 0 & 0 & v & v & \bar{v} & \bar{v} \\ v & \bar{v} & 0 & \bar{0} & 0 & 0 & 0 & 0 & 0 & 0 & 0 & 0 \\ 0 & 0 & w & \bar{w} & 0 & 0 & 0 & 0 & 0 & 0 & 0 & 0 \\ 0 & 0 & 0 & 0 & x & \bar{x} & 0 & \bar{0} & 0 & 0 & 0 & 0 \\ 0 & 0 & 0 & 0 & 0 & 0 & y & \bar{y} & 0 & \bar{0} & 0 & 0 \\ 0 & 0 & 0 & 0 & 0 & 0 & 0 & z & z & 0 & 0 \end{bmatrix} \quad \text{(g)}$$

Orthogonal matrix for 1024gray shades:

$$\begin{bmatrix}
b & b & b & b & b & b & b & b & 0 & 0 & 0 & 0 \\
0 & 0 & 0 & 0 & 0 & 0 & 0 & 0 & b & b & b & b \\
c & c & \overline{c} & \overline{c} & 0 & 0 & 0 & 0 & 0 & 0 & 0 & 0 \\
0 & 0 & 0 & 0 & d & d & \overline{d} & \overline{d} & 0 & 0 & 0 & 0 \\
0 & 0 & 0 & 0 & 0 & 0 & 0 & 0 & v & v & \overline{v} & \overline{v} \\
0 & 0 & v & \overline{v} & 0 & 0 & 0 & 0 & 0 & 0 & 0 & 0 \\
0 & 0 & 0 & 0 & w & \overline{w} & 0 & 0 & 0 & 0 & 0 & 0 \\
0 & 0 & 0 & 0 & 0 & 0 & x & \overline{x} & 0 & 0 & 0 & 0 \\
0 & 0 & 0 & 0 & 0 & 0 & 0 & 0 & y & \overline{y} & 0 & 0 \\
0 & 0 & 0 & 0 & 0 & 0 & 0 & 0 & 0 & 0 & z & \overline{z}
\end{bmatrix}$$

(h)

Orthogonal matrix for 2048 gray shades:

$$\begin{bmatrix}
b & b & b & b & b & b & b & b & b & b & b & b & b & b & b & b \\
c & c & c & c & c & c & c & c & c & c & c & c & c & c & c & c \\
c & c & c & c & \overline{c} & \overline{c} & \overline{c} & \overline{c} & 0 & 0 & 0 & 0 & 0 & 0 & 0 & 0 \\
0 & 0 & 0 & 0 & 0 & 0 & 0 & 0 & 0 & 0 & 0 & 0 & c & c & \overline{c} & \overline{c} \\
0 & 0 & 0 & 0 & 0 & 0 & 0 & 0 & d & d & \overline{d} & \overline{d} & 0 & 0 & 0 & 0 \\
0 & 0 & 0 & 0 & v & v & \overline{v} & \overline{v} & 0 & 0 & 0 & 0 & 0 & 0 & 0 & 0 \\
w & w & \overline{w} & \overline{w} & 0 & 0 & 0 & 0 & 0 & 0 & 0 & 0 & 0 & 0 & 0 & 0 \\
0 & 0 & 0 & 0 & 0 & 0 & 0 & 0 & w & \overline{w} & 0 & 0 & 0 & 0 & 0 & 0 \\
0 & 0 & 0 & 0 & 0 & 0 & 0 & 0 & 0 & 0 & x & \overline{x} & 0 & 0 & 0 & 0 \\
0 & 0 & 0 & 0 & 0 & 0 & 0 & 0 & 0 & 0 & 0 & 0 & y & \overline{y} & 0 & 0 \\
0 & 0 & 0 & 0 & 0 & 0 & 0 & 0 & 0 & 0 & 0 & 0 & 0 & 0 & z & \overline{z}
\end{bmatrix}$$

(i)

Orthogonal matrix for 4096 gray shades:

$$\begin{bmatrix}
a & \overline{a} & a & \overline{a} & a & \overline{a} & a & \overline{a} & a & a & a & a & a & a & a & a \\
b & b & b & b & b & b & b & b & b & b & b & b & b & b & b & b \\
b & b & b & b & \overline{b} & \overline{b} & \overline{b} & \overline{b} & 0 & 0 & 0 & 0 & 0 & 0 & 0 & 0 \\
0 & 0 & 0 & 0 & 0 & 0 & 0 & 0 & 0 & 0 & 0 & 0 & b & b & \overline{b} & \overline{b} \\
0 & 0 & 0 & 0 & 0 & 0 & 0 & 0 & c & c & \overline{c} & \overline{c} & 0 & 0 & 0 & 0 \\
0 & 0 & 0 & 0 & d & d & \overline{d} & \overline{d} & 0 & 0 & 0 & 0 & 0 & 0 & 0 & 0 \\
d & \overline{d} & 0 & 0 & 0 & 0 & 0 & 0 & 0 & 0 & 0 & 0 & 0 & 0 & 0 & 0 \\
0 & 0 & v & \overline{v} & 0 & 0 & 0 & 0 & 0 & 0 & 0 & 0 & 0 & 0 & 0 & 0 \\
0 & 0 & 0 & 0 & 0 & 0 & 0 & 0 & w & \overline{w} & 0 & 0 & 0 & 0 & 0 & 0 \\
0 & 0 & 0 & 0 & 0 & 0 & 0 & 0 & 0 & 0 & x & \overline{x} & 0 & 0 & 0 & 0 \\
0 & 0 & 0 & 0 & 0 & 0 & 0 & 0 & 0 & 0 & 0 & 0 & y & \overline{y} & 0 & 0 \\
0 & 0 & 0 & 0 & 0 & 0 & 0 & 0 & 0 & 0 & 0 & 0 & 0 & 0 & z & \overline{z}
\end{bmatrix}$$

(j)

Legend:

$a = 16,\ b = 8\sqrt{2},\ \overline{b} = -8\sqrt{2}, c = 8,\ \overline{c} = -8,$

$d = 4\sqrt{2},\ \overline{d} = -4\sqrt{2},\ v = 4,\ \overline{v} = -4,$

$w = 2\sqrt{2},\ \overline{w} = -2\sqrt{2},\ x = 2,\ \overline{x} = -2,$

$y = \sqrt{2}, \overline{y} = -\sqrt{2},\ z = 1,\ \overline{z} = -1$

Raghavasimhan Thirunarayanan is a visiting student at the Raman Research Institute. He obtained his B.E. in electrical and electronics from the Birla Institute of Technology and Science, Pilani, India.

Temkar N. Ruckmongathan obtained his B.E. in electronics and communication from the University of Madras, M.E. and Ph.D. degrees in electrical communication engineering from the Indian Institute of Science, Bangalore, India, in 1976, 1978, and 1988, respectively. Driving-matrix liquid-crystal displays has been his main field of study. He is a Professor at the Raman Research Institute, Bangalore, India. He was a Visiting Professor at Chalmers University of Technology, Sweden, during 1998, Guest Researcher at Asahi Glass Co. R&D at Yokohama, Japan, from 1991 to 1993 and LCD specialist at Philips, Heerlen, The Netherlands from 1989 to 1991. His pioneering work on multi-line addressing techniques is cited in about 90 U.S. patents. The analysis presented in the paper entitled "A generalized addressing technique for RMS responding LCDs" (presented at the International Display Research Conference in 1988), holds good for most of the multi-line addressing techniques. His main interest is in the research and development of new addressing techniques for driving-matrix LCDs. He is a Senior Member of the Society for Information Display.